An Experimental Study of Bubble Deformation in Viscous Liquids in Simple Shear Flow

Eduardo L. Canedo, Moshe Favelukis, Zehev Tadmor, and Yeshayahu Talmon
Dept. of Chemical Engineering, Technion-Israel Institute of Technology, Haifa 32000, Israel

An experimental study of the deformation of gas bubbles in viscous Newtonian liquids subjected to simple shear flow has been undertaken as a first step toward understanding bubble dynamics in polymer processing. Measurements of the shape, interfacial area, and volume of air bubbles suspended in the gap between two coaxial, counterrotating cylinders are presented and discussed as function of capillary number. At high capillary numbers (high deformations), the experiments confirm the theoretical model of Hinch and Acrivos.

Introduction

In the chemical processing industries, mass transfer between liquids and gases is often conducted in systems in which the gas phase is dispersed into a continuous liquid phase in the form of a swarm of bubbles. Thus, the analysis of bubble dynamics has a long history and an enduring place in the chemical engineering sciences. Most of the present knowledge on bubble growth and dissolution is restricted to ordinary, low-viscosity Newtonian liquids, under relatively shear-free environments. Very little is known about the effect of shear fields in these processes. However, high-viscosity liquids such as polymer melts, foods, and biological materials are usually processed under conditions in which high shear rates develop. Modeling of processes such as foam-enhanced polymer melt devolatilization (Biesenberger and Sebastian, 1983) requires a quantitative understanding of mass-transfer-driven bubble formation, growth, and dissolution in sheared liquids.

There is some evidence that shear fields have a pronounced effect on bubble formation. Harvey et al. (1944) proposed a mechanism for the release of microbubbles from suspended microscopic dust particles, in which shear played a key role. This type of mechanism has been advocated as the principal source of bubbles during the devolatilization of polymer melts in rolling pools (Biesenberger and Lee, 1986). However, it is not clear to what extent shear fields might affect the growth or dissolution of bubbles already suspended in a liquid.

Consider the case of an isolated bubble suspended in a uniform viscous liquid, in thermal, but not in chemical, equilibrium with the gas or vapor inside the bubble. Typical cases are the dissolution of a sparingly soluble gas bubble in an unsaturated liquid, and the growth of a vapor bubble in a dilute, supersaturated solution. We use here the terms "vapor bubble" and "gas bubble" as practically equivalent, in contrast to the definite, often opposed, meanings they have in the cavitation and boiling literature.

An isolated bubble, growing or dissolving in a liquid otherwise at rest, adopts a spherical shape, if the minor effect of gravity can be neglected. The only motion in the liquid phase is the radial flow generated by the expansion or contraction of the bubble. In this case, mass transfer in the liquid proceeds by a combination of molecular diffusion and radial convection of the volatile solute to or from the bubble surface. Quite often the convective contribution may be neglected.

If a shearing motion is imposed on the liquid, we can imagine two different though interrelated effects. First, the shear fields change the shape of the bubble. Bubble deformation increases the interfacial area and affects the flow field around the bubble. Second, the mass-transfer mechanism is altered, because external forced convection should be taken into account. The convective contribution may be dominant and cannot be neglected *a priori*, even if the rate of bubble growth or dissolution is small.

The purpose of our work is to substantiate these qualitative features and to provide the experimental and theoretical basis for a quantitative estimate of the effect of shear on the rate of bubble growth or dissolution. This first communication addresses the problem of bubble deformation in Newtonian liquids subjected to simple (plane Couette) shear from an experimental point of view.

Correspondence concerning this article should be addressed to Y. Talmon.
Present address of E. L. Canedo: Farrel Corporation, Ansonia, CT 06401.

Background

There is a large body of literature on the subject of drop deformation in shear fields (Rallison, 1984). Most theoretical treatments consider the case of drops of arbitrary viscosity and are valid in the limit of inviscid drops, which in the present context are equivalent to bubbles. Most experimental results were obtained with immiscible liquid drops suspended in another liquid. The ratio of suspended or dispersed drop viscosity (μ') to suspending or continuous-phase viscosity (μ), $\lambda = \mu'/\mu$, spans the range from 10^{-6} to 10^{3}.

The basic assumptions of most theoretical calculations closely followed in the experimental studies are:

- Steady creeping flow with negligible inertial effects
- Incompressible Newtonian fluids, both suspending and suspended
- No buoyancy effects, negligible net body forces on the drop
- No wall effects, effectively unbounded suspending flowfield
- No heat or mass transfer, isothermal conditions; constant physical properties.

Let us assume a single bubble or inviscid drop ($\lambda \ll 1$) located at the origin of a Cartesian coordinate system. The undisturbed motion in the continuous phase, far away from the drop, is the simple shear flow or plane Couette flow:

$$u_x = \dot{\gamma} y$$

$$u_y = u_z = 0 \tag{1}$$

where $\dot{\gamma}$ is the (constant) shear rate. Dimensional analysis shows that the flow around the drop is completely determined by a single dimensionless parameter, Ca, the capillary number, that is, the ratio of the shear forces (which tend to deform the drop) to the surface tension forces (which tend to keep the drop spherical):

$$Ca = \frac{\tau a}{\sigma} = \frac{\mu \dot{\gamma} a}{\sigma} \tag{2}$$

τ is a characteristic shear stress, a is the equivalent radius (radius of a sphere of equal volume), and σ is the surface tension.

Small deformations

For small deformations, $Ca \ll 1$, and if $\lambda \ll 1$, the bubble can be considered a slightly perturbed sphere, and an approximate solution of the creeping flow equations of motion (Stokes's equations) can be obtained by a regular perturbation technique.

Taylor (1932, 1934) obtained the $O(Ca)$ solution, later refined by Cox (1969); see also Hetsroni and Haber (1970). Chaffey et al. (1965, 1967) and Chaffey and Brenner (1967), and in a more general context Barthes-Biesel and Acrivos (1973) obtained $O(Ca^2)$ solutions. To $O(Ca)$ the drop is an ellipsoid oriented along the principal axis of deformation of the undisturbed flow (Figure 1), where l and b are the major and minor axes of the ellipse, $\alpha = 45°$ is the inclination angle, and D is the Taylor deformation parameter:

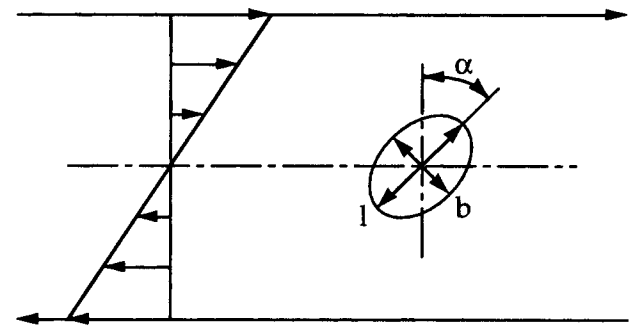

Figure 1. Deformation of a bubble in simple shear flow at $Ca \ll 1$.

$$D = \frac{l-b}{l+b} = Ca \tag{3}$$

To $O(Ca^2)$ this approach predicts an elongated shape with a "waist" in the middle and leaning in the direction of the flow.

The results of the $O(Ca)$ theory have been fully checked in experiments by Taylor (1934), Bartok and Mason (1959), Rumscheidt and Mason (1961), Karam and Bellinger (1968), Grace (1971), Torza et al. (1972), and others. It was found to be in excellent agreement with the experimental data up to Ca = 0.1. Some qualitative features of the $O(Ca^2)$ theory (change in drop shape and orientation) have been observed by these researchers at slightly higher values of the capillary number.

Large deformations

At high values of the capillary number, $Ca \gg 1$, and if $\lambda \ll 1$, a deformed drop cannot be considered a slightly perturbed sphere. In this situation, the slender-body theory for Stokes flow may be applied, as first suggested by Taylor (1964). The influence of the drop in the flow field is then represented by a distribution of singularities along its axis.

An approximate solution of the problem in simple shear flow was presented by Hinch and Acrivos (1980). It is based on the approximation that the cross-section of the drop is circular. Although this is not quite true, Hinch and Acrivos (1979) found that their results for two-dimensional hyperbolic flow, in which the cross-section of the drop is elliptical, give practically the same values of drop elongation and critical drop size as in the case of uniaxial extensional flow, in which the cross-section of the drop is circular, a case previously investigated by Acrivos and Lo (1978). According to Hinch and Acrivos (1980), the shape of the deformed drop is given by two functions: the position of the drop centerline $\eta(x)$, and the drop radius $R(x)$; see Figure 2.

For an inviscid drop, a case which ignores the variation of the pressure inside the drop, the dimensionless drop centerline $\eta^*(x)$ and radius $R^*(x)$ are:

$$\eta^* = \frac{\eta}{a} = \pm\sqrt{3}R^*(0)\left[1 - \left(\frac{R^*(x)}{R^*(0)}\right)^2\right]^{1/2} \tag{4}$$

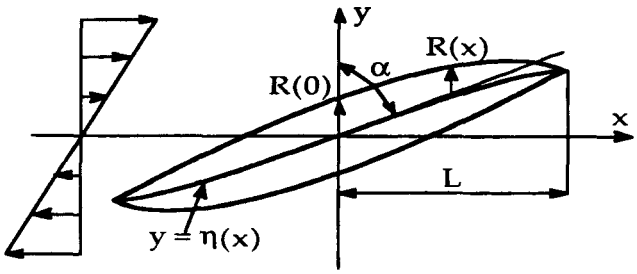

Figure 2. Deformation of a bubble in simple shear flow at $Ca \gg 1$.

$$x^* = \frac{x}{a} = \pm 2\sqrt{3}[R^*(0)]^2 Ca \times \left\{ \cos^{-1} \frac{R^*(x)}{R^*(0)} + \sqrt{2}\left[1 - \left(\frac{R^*(x)}{R^*(0)} \right)^2 \right]^{1/2} \right\} \quad (5)$$

$R^*(0)$ is the dimensionless radius at the center of the bubble, given by:

$$R^*(0) = \frac{R(0)}{a} = 0.578 Ca^{-1/4} \quad (6)$$

Other geometric parameters can be derived from Eqs. 4–6, for example, the half-length of the bubble, L^*:

$$L^* = \frac{L}{a} = 3.45 Ca^{1/2}, \quad (7)$$

the slenderness ratio:

$$\frac{R^*(0)}{L^*} = \frac{R(0)}{L} = 0.167 Ca^{-3/4}, \quad (8)$$

the inclination angle, α, the angle between the drop centerline and the y-axis at the bubble center:

$$\alpha = ctg^{-1}\left[\frac{d\eta(x)}{dx} \right]_{x=0} = ctg^{-1}(0.359 Ca^{-3/4}), \quad (9)$$

and the dimensionless bubble surface area, A^*:

$$A^* = \frac{A}{4\pi a^2} = \int_0^{L^*} R^*(x^*) dx^* = 1.41 Ca^{1/4}. \quad (10)$$

The dimensionless volume, V^*, is defined by:

$$V^* = \frac{V}{\frac{4}{3}\pi a^3} = 1. \quad (11)$$

Some numerical values are given in Table 1.

The theoretical analysis by Hinch and Acrivos (1980) predicts an S-shaped, long, thin bubble. At increasing capillary numbers the bubble becomes thinner, longer, its surface area increases, and it forms a larger angle with the y-axis. Till now, only qualitative experimental verification of the theoretical developments of Hinch and Acrivos on low viscosity drop deformation have been available.

Table 1. Bubble parameters as a function of the capillary number for $Ca \gg 1$ and $\lambda \ll 1$.

Ca	$R(0)/L$	α	A^*
1	0.17	70°	1.4
10	0.030	86°	2.5
100	0.0053	89°	4.5

Experimental Studies

Experimental system

Simple shear flow can be approximately realized in the narrow gap between coaxial rotating cylinders (Figure 3). If the two cylinders rotate in opposite directions, a stationary cylindrical layer is located at some point in the gap. When the thickness of the gap, ΔR, is relatively small compared to the mean radius, R_m, ($\Delta R/R_m \ll 1$), the constant shear rate is given approximately by:

$$\dot{\gamma} \approx (\Omega_1 + \Omega_2) \frac{R_m}{\Delta R}, \quad (12)$$

where Ω_1 and Ω_2 are the angular speeds of the inner and outer cylinders, respectively.

By manipulating $\Omega_1 + \Omega_2$ and Ω_1/Ω_2 independently, instead of Ω_1 and Ω_2, a range of shear rates is obtained, while a bubble freely suspended in the gap can be "frozen" to allow visual observation and photographic recording of its behavior from a fixed point. This type of Couette flow apparatus has been used in the past for the study of the dynamics of solid particles and liquid drops suspended in viscous liquids, notably by Mason and coworkers ("Mk.1" apparatus: Trevelyan and Mason, 1951; "Mk.2" apparatus: Bartok and Mason, 1957; "Mk.4" apparatus: Darabaner and Mason, 1967).

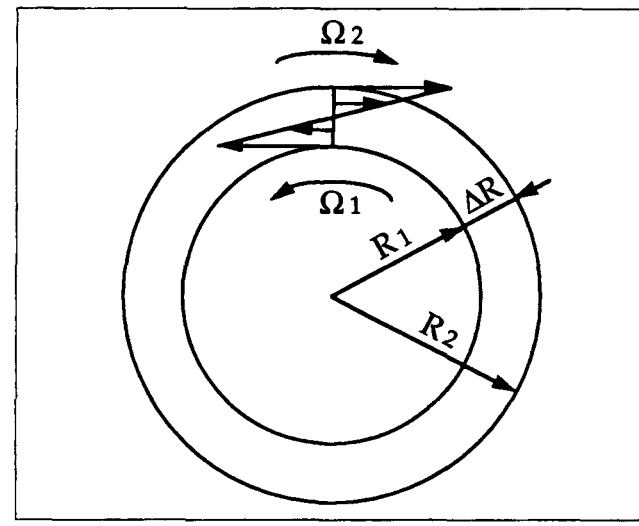

Figure 3. Couette flow apparatus.

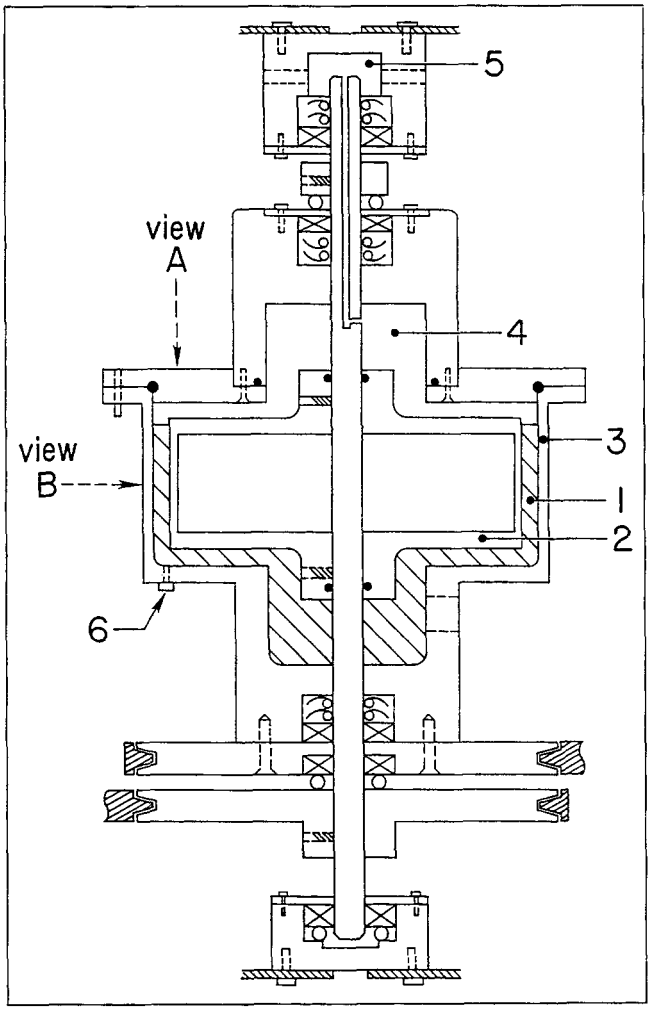

Figure 4. Experimental setup: (A) *x-y* plane view; (B) *x-z* plane view.

(1) liquid; (2) inner cylinder; (3) outer cylinder; (4, 5) vacuum space; (6) injection port.

We designed and constructed a Couette flow apparatus (CFA) following the above principles (Figure 4). It is composed of an inner stainless steel cylinder, 80 mm high, with a radius of 105.5 mm, and of an outer cylinder made of transparent acrylic plastic to facilitate illumination and observation. The radial gap between the cylinders is 9.3 mm. An injection port located at the bottom of the outer cylinder allows the introduction of gas bubbles into the gap. Two motors drive the cylinders in opposite directions, generating shear rates up to 20 s^{-1} in the gap between them.

The behavior of gas bubbles injected in the gap between cylinders was observed and photographed from the top and from the side. Two motorized 35-mm SLR cameras, focussed at approximately 1:1 to 1:2 magnification, were used to take simultaneous pictures from axial and radial viewpoints. The range of bubble sizes that could be studied with the system was limited by the width of the gap and visibility considerations to 0.1-3 mm in diameter.

Table 2. Physical properties of Chevron Polybutenes at 25°C

Material	ρ (kg/m^3)	μ (Pa·s)	σ (mN/m)
PB24	891	25.0	33.0
PB32	898	85.4	40.9

Materials

Air bubbles at atmospheric pressure measuring 1.5-3 mm in diameter were injected in several viscous liquids at ambient temperature. Low-molecular-weight polyisobutylenes (Chevron Polybutene 24 and 32) were chosen as typical high-viscosity Newtonian fluids. These materials (number-average molecular weight Mn = 950 and Mn = 1,400, respectively) behave as Newtonian liquids even at relatively high shear rates. Moreover, the low solubility of air in polyisobutylene leads to stable bubbles that facilitate observation. With this system, capillary numbers up to 50 could be obtained in the CFA. Viscosity and surface tension values were obtained from the literature (Chevron, 1980; Gaines, 1972) and checked in our laboratory (Cannon-Fenske capillary viscometer, Krüss tensiometer using the ring method). Relevant properties are presented in Table 2.

Technique

A typical run was conducted as follows: with the CFA filled with liquid, a small air bubble was introduced with a microsyringe into the gap between the cylinders through the injection port. Pictures of the undeformed bubble were taken at that point to determine the actual bubble size. Then, shear was applied and the bubble was "frozen" in place using the CFA speed-ratio control. Pictures of the deformed bubble were taken in the plane normal to the cylinder axis (*x-y* plane) and the plane tangent to the cylinder surface (*x-z* plane). After the motion of the cylinders had been discontinued, pictures of the undeformed bubble were taken again to check possible bubble dissolution (none was found). The temperature of the liquid was measured before and after each run; temperature increase on the order of 0.5°C was observed.

Negatives of the photographs of undeformed and deformed bubbles were projected on graph paper at large magnification, the bubble contours were traced, the lengths and the different radii of the bubble (along the *x*-axis) were measured, and interfacial area and volume were calculated. A more detailed description of the experimental technique can be found elsewhere (Favelukis, 1988).

Results and Discussion

Figures 5 and 6 show typical photographs of undeformed and deformed air bubbles in PB24 ($3 < Ca < 12$) and in PB32 ($7 < Ca < 48$). The difference in presentation between the two figures is because in Figure 5 the equivalent radii of all bubbles were the same, whereas in Figure 6 they were different. In the *x-y* plane, the boundaries of the inner and outer cylinders are clearly visible, and so is the typical S shape of the deformed bubble. It can also be seen that as the capillary number increases, the bubble becomes thinner and longer, and its angle with the *x* axis decreases as predicted by Hinch and Acrivos's theory. However, the photographs in the *x-z* plane show that the cross-section of the deformed bubble is not circular, as assumed by the theory, but is elliptical. Bubble radii at the center of the bubble were measured in the *x-y* plane, $R_1(0)$,

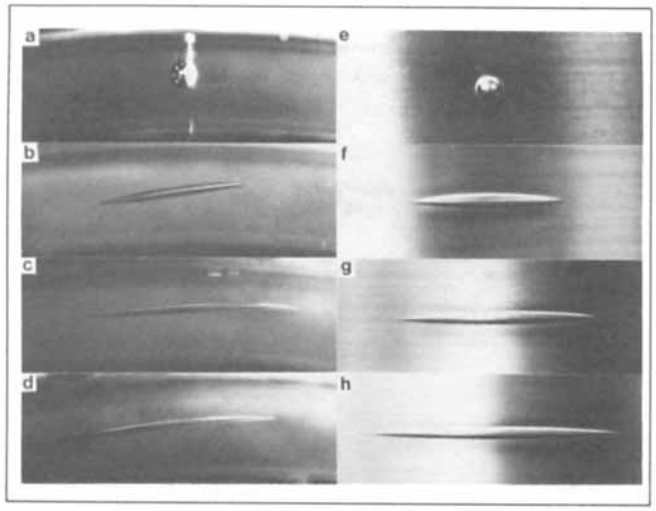

Figure 5. Deformed air bubbles in PB24 (equivalent radius in all photographs is 1.2 mm).

x-y plane: (a) $Ca=0$; (b) $Ca=3.9$; (c) $Ca=8.0$; (d) $Ca=11$; *x-z* plane: (e) $Ca=0$; (f) $Ca=3.8$; (g) $Ca=6.0$; (h) $Ca=11$.

and in the *x-z* plane, $R_2(0)$. The measurements expressed in dimensionless terms can be correlated by:

$$R_1^*(0)=0.52Ca^{-0.24} \tag{13}$$

$$R_2^*(0)=0.75Ca^{-0.24} \tag{14}$$

See Figure 7a. Note that the ratio $R_2^*(0)/R_1^*(0)$ is practically independent of the capillary number and is equal to 1.4. The experimentally evaluated exponents of the capillary number are almost the same as those predicted by the theory. The significant ellipticity observed in the deformed bubbles (undeformed bubbles are spherical) may be an intrinsic feature of a true linear, unbounded shear field, or could be a result of curvature of the system or wall effects. This point needs further exploring.

Figure 7b presents the dimensionless bubble half-length (L^*) as the function of Ca. The experimental results are somewhat lower than the predicted values. The dimensionless surface area (A^*) vs. capillary number is given in Figure 7c. Here, the agreement between the theory and the experiments is much better. Finally, Figure 7d shows the dimensionless volume (V^*), computed from the experimental measurements as function of Ca. Considering the fact that the error in calculating the volume from the measured dimensions is much greater than the error of the other parameters, the assumption of incompressible fluid in the bubble is correct. The last three parameters can be correlated in dimensionless terms by the following expressions:

$$L^*=3.1Ca^{0.43} \tag{15}$$

$$A^*=1.4Ca^{0.19} \tag{16}$$

$$V^*=0.92 \tag{17}$$

Experimental difficulties did not allow accurate measurement of the bubble inclination angle, α. In all cases, however, the deformed bubbles were found to be very stable, and no bubble fracture or breakup was observed. Sudden changes in shear stress had no apparent effect on bubble stability.

In conclusion, the theoretical analysis of Hinch and Acrivos (1980) for a slender-body bubble can be used to predict the geometrical parameters of such a bubble suspended in a viscous Newtonian liquid in simple shear flow. Reasonably good agreement between theory and experiments is expected for relatively large deformations, where the capillary number is in the range of $3<Ca<50$.

Acknowledgment

This research was supported in part by a grant from the National Council for Research and Development, Israel, and the Kernforschungsanlage, Jülich, Germany. We wish to thank Prof. A. Nir of the Technion and Prof. H. G. Fritz, of the Institut für Kunstofftechnologie (IKT), Stuttgart, for useful discussions and productive cooperation in this project. MF would like to thank the Gutwirth Fellowship Fund for its generous support. Finally, we thank Ms. Judith Schmidt for her help in preparing this manuscript.

Notation

a = equivalent radius of a bubble
A = surface area of a deformed bubble
b = minor axis of a deformed bubble
Ca = capillary number
D = Taylor deformation parameter
l = major axis of a deformed bubble
L = half-length of a deformed bubble
R = radius of the cylinder, radius of a deformed bubble
ΔR = thickness of the gap between the cylinders
u = velocity of the unperturbed flow field
V = volume of a deformed bubble

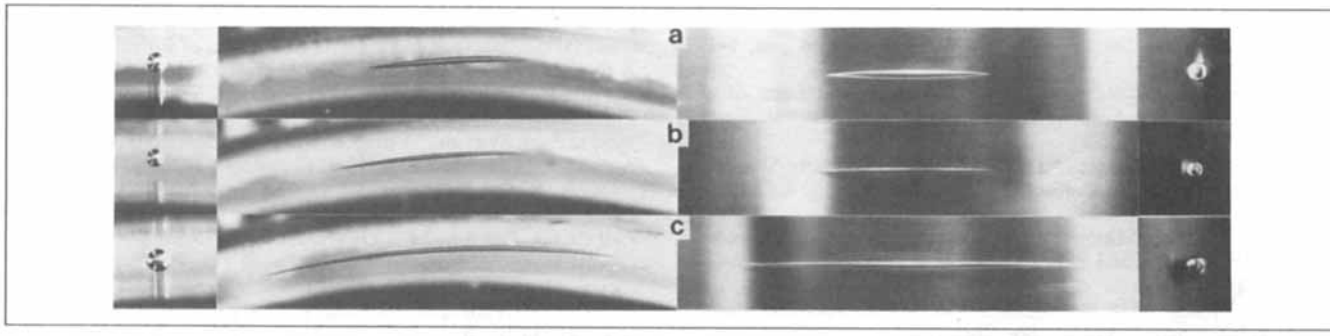

Figure 6. Deformed air bubbles in PB32 (*x-y* plane on the left and *x-z* plane on the right).

(a) $a=1.2$ mm, $Ca=7.1$; (b) $a=1.1$ mm, $Ca=18$; (c) $a=1.5$ mm, $Ca=41$.

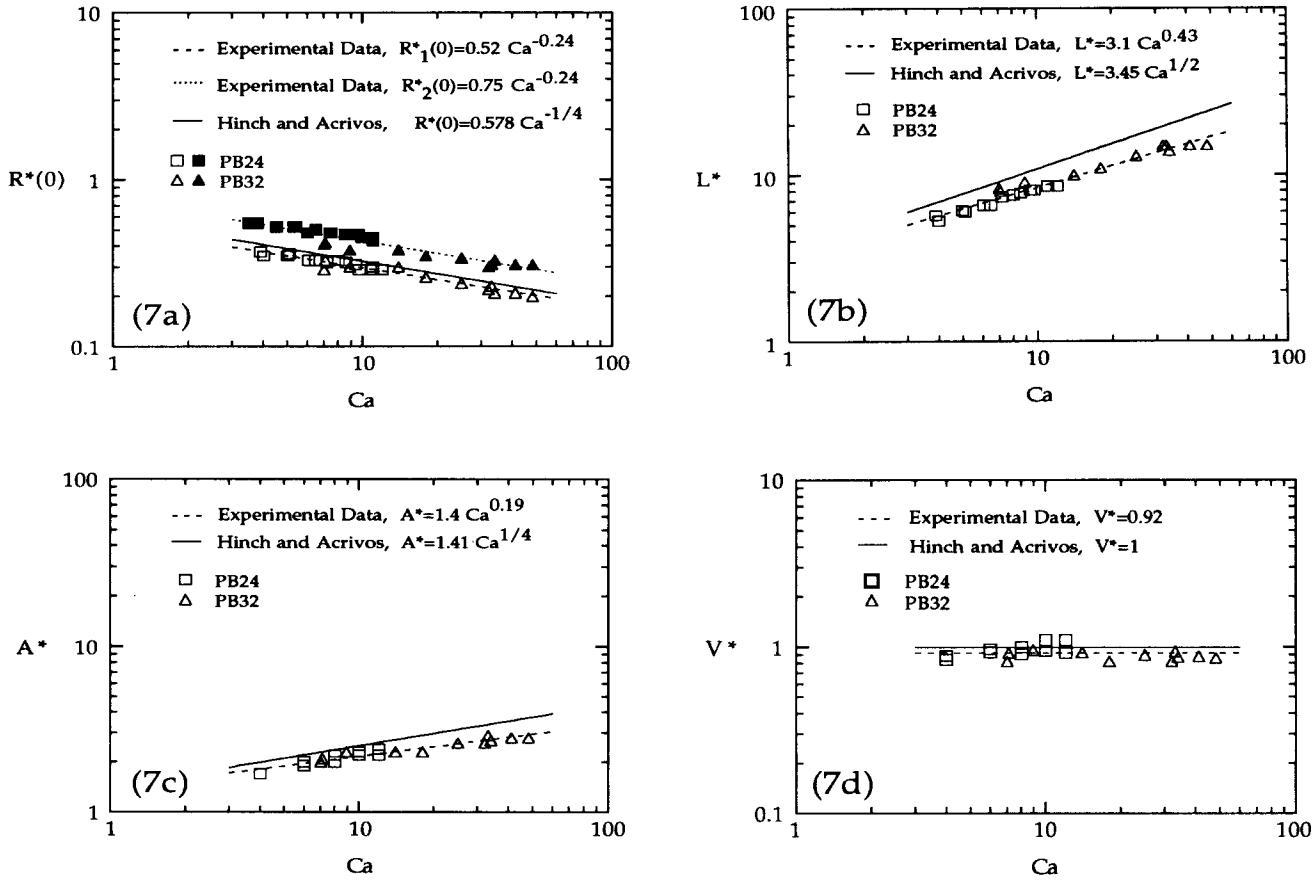

Figure 7. Deformation of air bubbles as function of *Ca* number: (a) dimensionless radii at bubble center; (b) dimensionless bubble half-length; (c) dimensionless bubble surface area; (d) dimensionless bubble volume.

Greek letters

α = inclination angle of a deformed bubble
$\dot{\gamma}$ = shear rate of the unperturbed flow
η = centerline position of a deformed bubble
λ = ratio of viscosities, dispersed to continuous phase
μ = viscosity of continuous phase (liquid)
μ' = viscosity of dispersed phase (bubble)
ρ = density of the continuous phase
σ = surface tension
τ = shear stress of unperturbed flow
Ω = angular speed of the cylinder

Literature Cited

Acrivos, A., and T. S. Lo, "Deformation and Breakup of a Single Slender Drop in an Extensional Flow," *J. Fluid Mech.*, **86**, 641 (1978).

Barthes-Biesel, D., and A. Acrivos, "Deformation and Burst of a Liquid Droplet Freely Suspended in a Linear Shear Field," *J. Fluid Mech.*, **61**, 1 (1973).

Bartok, W., and S. G. Mason, "Particle Motions in Sheared Suspensions: V. Rigid Rods and Collision Doublets of Spheres," *J. Colloid Sci.*, **12**, 243 (1957).

Bartok, W., and S. G. Mason, "Particle Motions in Sheared Suspensions: VIII. Singlets and Doublets of Fluid Spheres," *J. Colloid Sci.*, **14**, 13 (1959).

Biesenberger, J. A., and D. H. Sebastian, *Principles of Polymerization Engineering*, Chap. 6, Wiley, New York (1983).

Biesenberger, J. A., and S. T. Lee, "A Fundamental Study of Polymer Melt Devolatilization: II. A Theory of Foam-Enhanced DV," Technical Conf., Soc. of Plastics Engrs., SPE Tech. Papers 32, 846 (1986).

Chaffey, C. E., H. Brenner, and S. G. Mason, "Particle Motions in Sheared Suspensions: XVIII. Wall Migration (Theoretical)," *Rheol. Acta*, **4**, 64 (1965); *ibid.*, **6**, 100 (1967).

Chaffey, C. E., and H. Brenner, "A Second-Order Theory for Shear Deformation of Drops," *J. Colloid Interf. Sci.*, **24**, 258 (1967).

Chevron Chemical Co., "Chevron Polybutenes," product bulletin (1980).

Cox, R. G., "The Deformation of a Drop in a General Time-Dependent Fluid Flow," *J. Fluid Mech.*, **37**, 601 (1969).

Darabaner, C. L., and S. G. Mason, "Particle Motions in Sheared Suspensions: XXII. Interaction of Rigid Spheres (Experimental)," *Rheol. Acta*, **6**, 273 (1967).

Favelukis, M., "Dissolution of Gas Bubbles in Viscous Shear Flows," MSc Thesis, Dept. of Chemical Engineering, Technion-Israel Institute of Technology, Haifa (1988).

Gaines, G. L., "Surface and Interfacial Tension of Polymer Liquids: A review," *Polym. Eng. Sci.*, **12**, 1 (1972).

Grace, H. P., "Dispersion Phenomena in High Viscosity Immiscible Fluid Systems and Application of Static Mixers as Dispersion Devices in Such Systems," Engineering Foundation Conf. on Mixing, Andover NH (1971); *Chem. Eng. Commun.*, **14**, 225 (1982).

Harvey, E. N., D. K. Barnes, W. D. McElroy, A. H. Whiteley, D. C. Peace, and K. W. Cooper, "Bubble Formation in Animals," *J. Cell Comp. Physiol.*, **24**, 1 (1944); *J. Amer. Chem. Soc.*, **68**, 2119 (1946); *J. Appl. Phys.*, **18**, 162 (1947).

Hetsroni, G., and S. Haber, "The Flow in and around a Droplet or Bubble Submerged in an Unbound Arbitrary Velocity Field," *Rheol. Acta*, **9**, 488 (1970).

Hinch, E. J., and A. Acrivos, "Steady Long Slender Droplets in Two-Dimensional Straining Motion," *J. Fluid Mech.*, **91**, 401 (1979).

Hinch, E. J., and A. Acrivos, "Long Slender Drops in a Simple Shear Flow," *J. Fluid Mech.*, **98**, 305 (1980).
Karam, H. J., and J. C. Bellinger, "Deformation and Breakup of Liquid Droplets in a Simple Shear Field," *Ind. Eng. Chem. Fundam.*, **7**, 576 (1968).
Rallison, J. M., "The Deformation of Small Viscous Drops and Bubbles in Shear Flows," *Ann. Rev. Fluid Mech.*, **16**, 45 (1984).
Rumscheidt, F. D., and S. G. Mason, "Particle Motions in Sheared Suspensions: XII. Deformation and Burst of Fluid Drops in Shear and Hyperbolic Flow," *J. Colloid Sci.*, **16**, 238 (1961).
Taylor, G. I., "The Viscosity of a Fluid Containing Small Drops of Another Fluid," *Proc. Roy. Soc. (London)*, **A138**, 41 (1932).
Taylor, G. I., "The Formation of Emulsions in Definable Fields of Flow," *Proc. Roy. Soc. (London)*, **A146**, 501 (1934).
Taylor, G. I., "Conical Free Surfaces and Fluid Interfaces," *Proc. Int. Cong. of Appl. Mech.*, p. 790, Munich, Springer-Verlag (1964).
Torza, S., R. G. Cox, and S. G. Mason, "Particle Motions in Sheared Suspensions: XXVII. Transient and Steady Deformation and Burst of Liquid Drops," *J. Colloid Interf. Sci.*, **38**, 395 (1972).
Trevelyan, B. J., and S. G. Mason, "Particle Motions in Sheared Suspensions: I. Rotations," *J. Colloid Sci.*, **6**, 354 (1951).

Manuscript received Nov. 13, 1991, and revision received Sept. 14, 1992.